Molecular characteristics of an adhesion molecule containing cholesterol-dependent cytolysin-motif produced by Mitis group streptococci

松本　愛理

TABLE OF CONTENT

CHAPTER 1. Background

From the cumulative *de novo* genomic information in recent years, distribution and feature of various virulence factors is becoming clearer even in the Mitis group streptococci (MGS) that is resident in the human pharynx and oral cavity. One of them is a pore-forming toxin produced by gram-positive bacteria showing pathogenicity, such as cholesterol-dependent cytolysins (CDCs) (1) that recognize cell-membrane cholesterol of target cells as a receptor. According to the results from various research conducted by many researchers around the world including our group, it has been revealed that each domain of typical 4-domains type of CDCs has its individual role in the formation of membrane pores on the target cell membrane: The domain 1 functions to maintain the adequate three-dimensional position between the domain 2 and the domain 3, and contribute to the oligomer assembly (2). The domain 2 is considered to be the backbone structure of CDC (2). The domain 3 contains the components that form a membrane-penetrating structure by changing their structure from α-helix to β-sheet (2, 3). Finally, the domain 4 functions as a membrane-binding domain in the first step of toxin-cell interaction (2, 4). Interestingly, the CDC produced from MGS has unique structural variety, such as an additional functional domain (ExD) at the N-terminal of 5-domains-type CDCs (5, 6). Furthermore, the receptor recognition diversity in CDCs was revealed by the discovery of CDCs including 5-domains-type CDCs that recognize both cholesterol and human CD59, a GPI anchor protein as a receptor (7, 8). However, the details of their molecular functions and relevance to the pathogenicity have been still remaining unclear. Judging from these facts, MGS-derived CDCs seems to have outstanding structural and functional diversity that is never found in streptococcal typical CDCs. On the background mentioned above, we are interested in MGS-derived CDCs including the related molecules and decided to conduct the research on them.

Streptococcus pseudopneumoniae (SPpn) is a relatively new species belonging to the

MGS proposed in 2004 (9). According to the comparative genomic analysis, SPpn is closely related to *Streptococcus pneumoniae* (SPn) and *Streptococcus mitis* (SM), which belongs to the MGS (10). SPn is a well-known pathogen of humans responsible for the disorders such as otitis media, meningitis, pneumonia, and sepsis (11, 12). Generally, although other species of MGS, including SPpn, have been considered opportunistic pathogens with low pathogenicity against humans, the clinical significance as the causative agent of various infections such as endocarditis, and fulminant infection is emerging in MGS (13-15). Regarding the pathogenicity of SPpn, it has been reported that SPpn showed potential pathogenicity, such as in an experimental mouse peritonitis/sepsis model (16), suggesting relevance to the history or exacerbation of chronic obstructive pulmonary disease (COPD) (17) and in human fatal septicemia (15). Moreover, with regard to virulence factors, it is known that the genes encoding various pneumococcal virulence factors are present in the SPpn genome (18). For example, a homolog of pneumolysin (PLY) (19) named pseudopneumolysin (PPLY) (20) is present in the SPpn genome. In addition to PPLY, another gene encoding the homolog of lectinolysin (LLY), atypical 5-domains-type CDC possessing N-terminal additional domain with lectin activity (6), has been reported (21). Furthermore, a novel open reading frame (ORF) deduced to encode a unique CDC-like molecule showing plural gene-fused and never reported feature with a molecular weight of ~100 kDa was revealed in the genome of SPpn strain IS7493 in addition to the genes encoding PPLY and LLY homolog (21). Although SPpn possesses and produces the pathogenic factors and candidate molecules of pathogenic factors described above, their contribution to pathogenicity is still unclear. Therefore, further investigation on the virulence factors of SPpn, particularly the novel CDC-like molecule with no information in protein level, is necessary to understand the characteristics of SPpn such as its significance in medical aspect.

CHAPTER 2. Introduction

A novel ORF presumed to encode a CDC-like molecule was reported in the genome of SPpn strain IS7493 (21). Based on its nucleotide sequence information, the product of this novel gene was predicted to may have multiple functions due to the finding that a lipase domain (lipase_3), tandem-arranged F5_F8_type_C domains, and a receptor-recognition domain of the CDC (thiol cytolysin domain) were present in the molecule (21). However, the expression of this predicted molecule with multiple functional domains in SPpn and the molecular function has not yet been confirmed to date.

In the present study, we investigated the distribution of this gene encoding the protein with multiple functional domains among the oral streptococci. Subsequently, the expression of the gene in the strains with this novel gene was confirmed by detecting the transcription-translation product using ELISA and immunoblotting technique. In addition, the functions of the translated products were characterized using various recombinants derived from this protein. Consequently, it was revealed that the gene encoding this protein was distributed among the strains belonging to MGS. Moreover, the encoded protein showed multiple functions, especially lectin activity giving host cell-binding property to the bacteria. Thus, we named this multi-functional protein as “mitilectin (MLC)”, and investigated its role in the pathogenicity of MLC-producing oral streptococci.

CHAPTER 3. Materials and Methods

1. Distribution of the gene encoding mitilectin among streptococcal species

1.1 Identification of mitilectin-positive streptococci in online databases

Streptococcal strains possessing the gene encoding MLC were searched in the NCBI database using BLAST (https://blast.ncbi.nlm.nih.gov/Blast.cgi) and also searched among the stock strains in our laboratory. The amino acid sequence of MLC was aligned using Clustal X (http://www.clustal.org/clustal2/).

1.2 Phylogenetic analysis using a multi-locus sequence typing

The two strains registered as *Streptococcus oralis* subsp. *dentisani* found in the web database (https://blast.ncbi.nlm.nih.gov/Blast.cgi), were re-evaluated using the multi-locus sequence typing (MLST) method for the classification of SPn (22).

2. Preparation of recombinant mitilectins

2.1 Bacterial strains and culture conditions

The bacterial strains used in this study were SPpn type strain ATCC BAA-960 ($SPpn^T$), SM Nm-65 isolated from the tooth surface of a patient with Kawasaki disease (23), and SM type strain NCTC12261 (SM^T). These strains were cultured at 37 °C under a 5% CO_2 atmosphere. Brain-heart infusion (BHI; Becton Dickinson and Company, Franklin Lakes, NJ, USA) broth supplemented with 5% (v/v) heat-inactivated horse serum (HS) was used for the culture medium. *Escherichia coli* BL21 (DE3) pLysS was grown in Luria-Bertani (LB) broth at 37 °C. If needed, antibiotics were added at the following final concentrations: ampicillin (Amp) at 50 μg/mL and chloramphenicol (CP) at 34 μg/mL.

2.2 Preparation of the recombinant mitilectins

In order to prepare the expression vector for N-terminal His-tagged rMLC (abbreviated hereafter as His-rMLC), the gene encoding MLC with deleted 5'-terminal 108 bp sequence encoding the secretion signal, searched on SignalP-5.0 (http://www.cbs.dtu.dk/services/SignalP/), was amplified using the genomic DNA prepared from $SPpn^T$ as the template. The primers, viz., mitilectin F and mitilectin R, have been provided in Table 1. Amplification was carried out in 35 cycles of denaturation at 98 °C for 10 s, annealing at 55 °C for 5 s, and extension at 72 °C for 160 s. The coding sequence of the N-terminal His-tagged vector pETHis (National Institute of Genetics, Shizuoka, Japan) was also amplified by inverse PCR using PrimeSTAR HS DNA polymerase (TaKaRa Bio Inc., Shiga, Japan), and the primers In-F his F and In-F his R (Table 1) were used. The amplified fragment encoding MLC was cloned into the amplified pETHis using the In-Fusion HD cloning kit (TaKaRa Bio Inc.) at 50 °C for 15 min. The constructed plasmid (pETHisMLC) was introduced into BL21 (DE3) pLysS by heat shock method as follows: a mixture of the strain and the vector was incubated on ice for 30 min, heated at 42 °C for 30 s, and then quickly placed on ice. After transformation and recovery of the culture, transformants were selected on LB agar containing 50 μg/mL Amp and 34 μg/mL CP after overnight incubation. Screening of the target clones was conducted using direct colony PCR with the primers seq F, seq R, and Lipase R (Table 1), following the PCR program with 30 cycles of denaturation at 95 °C for 30 s, annealing at 50 °C for 30 s, and extension at 72 °C for 3 min. The constructed expression vector was purified from the selected clone cultured in LB broth containing 50 μg/mL Amp and 34 μg/mL CP using NucleoSpin Plasmid EasyPure (TaKaRa Bio Inc.), and sequenced (Eurofins Genomics K.K., Tokyo, Japan).

The selected clone was pre-cultured overnight in LB broth containing antibiotics. Subsequently, the expression of recombinant proteins were induced to the logarithmic growth phase by overnight incubation in the presence of 1 mM (final concentration) isopropyl

β-D-thiogalactopyranoside (IPTG) at 25 °C. The expressed His-rMLC was purified using nickel-affinity chromatography according to a previously reported method (24). Purified His-rMLC was subjected to SDS-PAGE and visualized using Coomassie Brilliant Blue (CBB) staining.

The construction of the expression system for rMLC mutants (Figure 1) was carried out by the PCR-based mutagenesis method using PrimeSTAR Max DNA polymerase (TaKaRa Bio Inc.) and primer sets described in Table 1. The purification of the constructed vectors and the confirmation of their sequence were also conducted as described above.

In addition to rMLCs described above, two recombinant CDCs, N-terminal His-tagged recombinants of *S. mitis*-derived human platelet aggregation factor (His-rSm-hPAF) and suilysin (His-rSLY) were prepared as reported previously (25), and used as reference CDCs for the comparison of hemolytic activity.

Table 1. Oligonucleotides used in this study

Purpose	Name	Sequence (5' to 3')
Construction of recombinant proteins	mitilectin F	CACCATCACCTCGAGAATGAACTAAAGCAAGATGTAAC
	mitilectin R	TTAGCAGCCGGATCCTTACAAGACATCGTCATCAG
	In-F his F	GGATCCGGCTGCTAACAAAGC
	In-F his R	CTCGAGGTGATGGTGATGGTG
	mutant ΔLF F	CCATCACCTCGAGACGCCTGTGAAA
	mutant ΔLF R	GTCTCGAGGTGATGGTGATGGTGATG
	mutant ΔFT F	AATGTAAGGATCCGGCTGCTAACAA
	mutant ΔFT R	CCGGATCCTTACATTGGTTCAGCGCT
	mutant ΔT F	TCAATAAGGATCCGGCTGCTAACAA
	mutant ΔT R	CCGGATCCTTATTGACTGATTGGTTG
	mutant ΔF F	ACCAATGCGCTTTATCGCTACGAAT
	mutant ΔF R	ATAAAGCGCATTGGTTCAGCGCTTGG
	H509A F	GTCACTGCTACAAACTTCCAATCTAAG
	H509A R	GTTTGTAGCAGTGACAGAATTGTGATC
	H643A F	AACACAGCTACTAAGTCTGAAAACCAA
	H643A R	CTTAGTAGCTGTGTTAGACTGTTGGCT
	R536A_R543A _R670A_R678A F	TACAACGCTACAGACACTGCCCAGGATGCTTTGGCAAA CTTTGATGTC
	R536A_R543A _R670A_R678A R	TGACAGAGCTTTGGAAACGTCTCCATCCCCAGCGTTAT GAAGGCGGACAAG
	In_F R536A_R543A _R670A_R678A F	CATAACGCTGGGGATGGAGACGTTTCCAAAGCTCTGTC AGACTTTGATGTG
	In_F R536A_R543A _R670A_R678A R	TGCCAAAGCATCCTGGGCAGTGTCTGTAGCGTTGTAAA TATTGATTTG
Construction of Δ*mlc* strain	MLC_up F	CCATTTATTCAGAGCTTTTC
	SacI_MLC_up R	AAAGAGCTCGGCTGAAATTCCAGCTGGAG
	SphI_MLC_dw F	AAAGCATGCAAAATCCTACTATTTAATAATGAGATGATT
	MLC_dw R	GTAATAAGAACGACCAGTGC
	cat F	AAAGAGCTCTCGAGAAGCTGGCAGATGTCC
	cat R	AAAGCATGCCAAGCTGTGACCGTCTCCGGGAGCTG
Sequencing	seq F	ATCGAGATCTCGATCCCGCG
	seq R	TCCTCCTTTCAGCAAAAAAC
	Lipase R	GTGTTTAAAGCGTGAATTAC

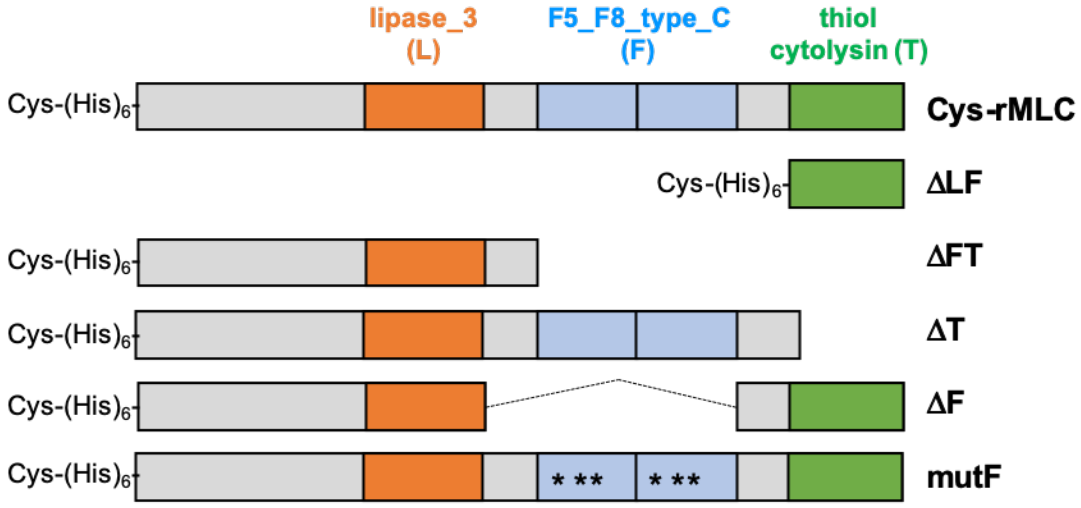

Figure 1. Schematic representation of recombinant MLCs used in this study. The N-terminal His-tagged and Cys residue-added recombinants of full-length MLC (Cys-rMLC), four deletion mutants (ΔLF, ΔFT, ΔT, and ΔF), and an Ala-substituted mutant with six substitutions: H509A, R536A, R543A, H643A, R670A, R678A in the F5_F8_type_C domain (mutF, the six mutations are shown as "★" in the scheme) were prepared. In all recombinants, one Cys residue was added to the N-terminal side of the molecule for the fluorophore labeling. In the scheme, boxes colored orange, blue, and green indicate lipase_3 domain (L), F5_F8_type_C domain (F), and thiol cytolysin domain (T), respectively.

3. Preparation of the anti-mitilectin serum

Anti-MLC serum (α-MLC) was prepared according to Protocol No. T29-38, approved by the Committee on Animal Experiments of Tokushima University (Tokushima, Japan). An emulsion of phosphate-buffered saline (PBS) containing His-rMLC (50 μg/mouse) and complete adjuvant (Adjuvant Complete Freund; FUJIFILM Wako, Osaka, Japan) was prepared and administered to BALB/c mice (female, >8 weeks; Japan SLC, Inc., Shizuoka, Japan) intraperitoneally as the first immunization. The second administration was performed 2 weeks after the first administration with the emulsion containing His-rMLC (50 μg/mouse) prepared using incomplete adjuvant (Adjuvant Incomplete Freund; FUJIFILM Wako). The α-MLC was obtained by centrifugation (800 × *g*, 5 min) of whole blood sampled from the euthanized mice after incubation at 37 °C for 1 h.

The pooled antiserum was validated for the titer and specificity against His-rMLC by enzyme-linked immunosorbent assay (ELISA) and immunoblotting. Briefly, for ELISA, 50 μL of 10 ng/μL His-rMLC in PBS was dispensed into each well of a 96-well microplate (PS, MICROLON, F-Bottom; Greiner Bio-One, Kremsmunster, Austria) and dried overnight at 37 °C. Blocking of wells was conducted by treatment with the blocking buffer for ELISA [PBS containing 1.0% (w/v) bovine serum albumin (BSA)] at 25 °C for 30 min. For antibody reaction, serial dilutions of α-MLC and 2,000-fold diluted HRP-conjugated goat anti-mouse IgG (SeraCare Life Sciences, Inc., MA, USA) were used as the primary and secondary antibodies, respectively. Each antibody reaction was performed at 25 °C for 1 h, followed by five rounds of PBS washes. After the final wash, the peroxidase substrate solution [2 mM 2, 2'-azino-bis (3-ethylbenzothiazolin-6-sulfonic acid) diammonium salt, 0.002% (v/v) H_2O_2, 50 mM $Na_2HPO_4 \cdot 12H_2O$] was dispensed into each well and incubated for 1 h at 25 °C. The absorbance of each well at 415 nm was measured using a microplate reader (Infinite M200, TECAN, Mannedorf, Switzerland). For immunoblotting, the optical density at 600 nm (OD_{600}) of 18 h SM^T culture was measured to estimate the dilution factor for adjusting its OD_{600} to 0.3, and the culture was centrifuged (13,000 × *g*, 5 min) to obtain the culture supernatant. Subsequently, the obtained culture supernatant was diluted with PBS according to the dilution factor estimated above. Then, 30 μL of the diluted culture supernatant (negative control) and the purified His-rMLC solution containing 10 ng of the protein (positive control) was mixed with 4-fold concentrated Laemmli's sample buffer, heated at 95 °C for 5 min, and subjected to SDS-PAGE in Laemmli's system. Subsequently, the separated proteins were transferred onto a polyvinylidene difluoride (PVDF) membrane (Immobilon-P transfer membrane; Merck Millipore, MA, USA) by semi-dry blotting. MLC was detected as follows: the transblotted membrane was blocked with blocking buffer for PVDF membranes [0.1% (v/v) Tween 20-containing Tris-buffered saline (TTBS) with 1.0% (w/v) of skim milk] at 25 °C for 1 h. Then, 300-fold diluted α-MLC and 5,000-fold diluted

HRP-conjugated goat anti-mouse IgG (SeraCare Life Sciences, Inc.) were used as the primary and secondary antibodies, respectively. Each antibody reaction was allowed to proceed at 25 °C for 1 h, followed by six rounds of TTBS washes. Finally, the obtained membrane was reacted with the substrate solution (Immobilon Western Chemiluminescent HRP Substrate; Merck Millipore), and MLC was detected using a LAS-4000mini EPUV (FUJIFILM, Tokyo, Japan).

4. Detection of the mitilectin produced by the tested strains

The OD_{600} of each 18 h bacterial culture was measured and the cultures were centrifuged (13,000 × *g*, 5 min) to separate the culture supernatant and cultured cells. Subsequently, the obtained culture supernatants were adjusted to the lowest OD_{600} among the tested cultures using PBS, and subjected to SDS-PAGE. The separated proteins were subsequently transferred onto a PVDF membrane by semi-dry blotting. Subsequently, the MLC was detected by immunoblotting as described above.

To detect MLC bound to the bacterial cell surface, the collected bacterial cells were washed with PBS. Subsequently, 50 μL of each bacterial cell suspension, with its OD_{600} adjusted to 0.1 by PBS, was dispensed into the wells of a 96-well plate. After overnight drying at 37 °C, MLC on the bacterial cell surface was detected by ELISA according to the method described in the previous section.

5. Characterization of the mitilectin function

5.1 Measurement of the hemolytic activity

Human erythrocytes were prepared from blood collected from a healthy volunteer under written informed consent in accordance with Protocol No. 15002 approved by the Institutional Ethics Review Board at the Institute of Technology and Science, Tokushima

University Graduate School, Japan. To measure the hemolytic activity, the preserved blood was centrifuged (800 × *g,* 5 min) to harvest erythrocytes. Subsequently, the erythrocytes were washed with PBS three times by centrifugation in the same condition and suspended in PBS to prepare a 50% (v/v) erythrocyte suspension. Washed erythrocytes were added to the reaction mixture containing 0.001–10 μg/ml (final concentration) His-rMLC in PBS at a final concentration of 0.5% (v/v). The sterilized deionized water was used instead of His-rMLC solution to prepare the complete hemolysis control, and PBS without His-rMLC was used to prepare the non-hemolysis control. In the present assay, His-rSm-hPAF and His-rSLY were used for comparison of hemolytic activity. Calculation of the hemolytic activity was performed as described previously (26).

5.2 Measurement of the lipase activity

Measurement of lipase activity of His-rMLC was performed using a Lipase Activity Assay Kit (Cayman Chemical, Ann Arbor, MI, USA) according to the manufacturer's protocol. Both His-rMLC and heat-denatured His-rMLC (hdMLC) were diluted to 0.1 μM with PBS. The heat denaturation of His-rMLC was performed at 96°C for 30 min.

5.3 Evaluation of the binding of recombinant mitilectins to HSC-2 cells

The human oral squamous cell carcinoma cell line HSC-2 (RCB1945, RIKEN BRC, Ibaraki, Japan) used in this study was cultured in Eagle's minimum essential medium containing 10% (v/v) of FBS. The fluorescent-labeled rMLCs were prepared as follows using recombinants with an N-terminal Cys residue (Cys-rMLC, ΔLF, ΔFT, ΔT, ΔF, mutF, Figure 1): 0.5 mg of each recombinant was incubated with Alexa Fluor 488 C5 maleimide (Invitrogen, Carlsbad, CA, USA) at a final concentration of 0.1 mM for 2 h at room temperature in the dark. After removal of the remaining unreacted fluorophore using a HiTrap desalting column (GE Healthcare, Chicago, IL, USA), each fluorescent-labeled rMLC was collected and used

for the assay. Prior to use in the binding assay, the ratio of fluorescent intensity per mole of each rMLC was adjusted to the same by mixing with the non-labeled rMLC.

HSC-2 cells suspended in culture medium were dispensed into 96-well plate wells at 4.0×10^4 cells/well and incubated overnight under cell culture conditions (37 °C, 5% CO_2 atmosphere). After exchanging the culture medium to EMEM without FBS, the fluorescent-labeled rMLCs were added at a final concentration of 0.1 μM and incubated for 30 min. Subsequently, the cells were washed twice with EMEM, and further incubated for overnight. Then, the morphology and the fluorescence on HSC-2 were observed using IN Cell Analyzer (GE Healthcare) or a fluorescent microscope (IX71, Olympus, Tokyo, Japan) equipped with CCD camera (DP72, Olympus). After observation, the cells were lysed with 1.0% (w/v) SDS, and the fluorescent intensity of each cell lysate was also measured (488 nm excitation wavelength, 530 nm emission wavelength) in a fluorescent microplate reader (Infinite M200, TECAN).

5.4 Evaluation of the binding of recombinant mitilectins to HL60 cells

The human promyelocytic leukemia cell line HL60 (RCB0041, RIKEN BRC) was cultured in RPMI1640 (FUJIFILM Wako) containing 10% (v/v) of FBS. HL60 cells were washed (800 × g, 3 min) twice with RPMI1640 and dispensed at 1.0×10^6 cells/100μL in 96-well cell-culture plate. The fluorescent-labeled rMLCs were added at a final concentration of 0.1 μM and incubated for 30 min under cell culture conditions (37 °C, 5% CO_2 atmosphere). Subsequently, the cells were washed twice with RPMI1640, and the fluorescence on the cells was evaluated using FACSVerse (Becton, Dickinson and Company, Tokyo, Japan).

5.5 Molecular modeling of the tandem-arranged F5_F8_type_C domain of mitilectin

A molecular model of the tandem-arranged F5_F8_type_C domain in MLC derived from $SPpn^T$ was constructed based on the X-ray data of lectinolysin (Protein Data Bank ID: 3LE0) using Insight II-Discover with homology module (Accelrys Inc., San Diego, CA, USA), as previously described (27, 28).

6. Evaluation of the mitilectin function in mitilectin-producing bacteria

6.1 Binding of mitilectin-producing bacteria to HSC-2 cells

HSC-2 was used as the target cell in this assay. The tested bacteria were labeled with 0.02 mM of PKH67 Green Fluorescent Cell Linker Midi Kit (Sigma-Aldrich, St. Louis, MO, USA) and washed, then resuspended to obtain a cell density of 4×10^6 cells/100 μL in EMEM. The same amount (100 μL) of α-MLC or control serum was added to the bacterial suspension and incubated for 1 h under cell culture conditions. After removal of the culture medium and twice washing with EMEM, 100 μL of bacterial suspension without PKH67-labeling was added to HSC-2 cells. After 3 h incubation, the culture supernatant was removed and the cells were washed twice with EMEM, then incubated for overnight. The fluorescence derived from the PKH67-labeled bacteria bound to or incorporated into HSC-2 cells was observed using IN Cell Analyzer 6000 (GE Healthcare) or a fluorescent microscope (IX71, Olympus) equipped with DP72 (Olympus). After the observation of HSC-2 cells, the cells were lysed with 1.0% (w/v) SDS and the fluorescence intensity of each lysate was measured (excitation wavelength for 488 nm, emission wavelength for 530 nm) with fluorescent microplate reader (Infinite M200, TECAN).

6.2 Construction of the gene deletion mutant encoding mitilectin derived from *Streptococcus mitis* strain Nm-65

The deletion mutant of the gene encoding MLC derived from *S. mitis* Nm-65 was constructed by the homologous recombination method in the presence of competence-stimulating peptide (CSP) according to a previously reported method (29). Briefly, the mutant strain possessing a chloramphenicol acetyltransferase (*cat*) gene cassette was generated as follows: to prepare the fragments for homologous recombination, PCR was performed using PrimeSTAR GXL DNA polymerase (TaKaRa Bio Inc.), purified genomic DNA from Nm-65 as the template, and primers for amplification of the upstream region of MLC (MLC_up F and SacI_MLC_up R, Table 1) and the downstream region of MLC (SphI_MLC_dw-F and MLC_dw-R, Table 1). The *cat* gene cassette was also amplified from the plasmid pMX2 (30) using PrimeSTAR GXL DNA polymerase (TaKaRa Bio Inc.) and the primer pair of cat F and cat R (Table 1). Subsequently, the amplified fragments were digested by restriction enzyme(s), SacI and/or SphI, then purified using the NucleoSpin Gel and PCR Clean-up (TaKaRa Bio Inc.). The purified fragments were ligated using a DNA Ligation Kit (TaKaRa Bio Inc.), and the fragment used for transformation was amplified by PCR using PrimeSTAR Max DNA polymerase (TaKaRa Bio Inc.) and primers (MLC_up F and MLC_dw R, Table 1) with the ligation mixture as the template. The transformation of Nm-65 with the prepared fragment was carried out in the presence of CSP, and transformants were selected on BHI agar plates containing 5% (v/v) horse defibrinated blood (Japan Bio Serum, Tokyo, Japan) in the presence of 4 μg/mL of CP.

Deletion of the target gene in the constructed mutant was confirmed by PCR using PrimeSTAR GXL DNA polymerase with the MLC_up F and MLC_dw R, and cat F and cat R primer sets (Table 1). The loss of MLC expression in the mutant was confirmed by immunoblotting with α-MLC.

7. Statistical analysis

Differences in experiments were evaluated using unpaired two-tailed Student's *t*-test. All data are presented as mean ± standard deviation (SD). Differences were considered significant when the probability value was calculated to be less than 5% ($p < 0.05$).

CHAPTER 4. Results

1. Distribution of the gene encoding mitilectin among streptococcal species

1.1 Streptococcal species possessing the gene encoding mitilectin and their homologs

Streptococcal species possessing the gene encoding a potentially multifunctional protein, mitilectin (abbreviated as MLC, this name is derived from the clarified distribution of the gene among the group of Streptococcal species and the molecular functions of the products revealed from this study and described in this section) with the 2,628 bp of ORF, and its homologous gene(s) on the genome were searched both on the BLAST web database (https://blast.ncbi.nlm.nih.gov/Blast.cgi) and among the stock strains in our laboratory. The transcriptional product from the MLC-encoding gene suggested to be possess an N-terminal secretion signal, lipase_3 domain, tandem structure of F5_F8_type_C lectin domain, and domain 4 of CDC (21). From the results of NCBI database search, *mlc* gene possessing strains were found mainly in the species of SPpn, SM, and SPn, all of the species belonging to MGS (Table 2). The rate of *mlc* gene possession in these species was as follows: SM, 25.0% (41/164); SPpn, 55.6%, (50/90); and SPn, 0.0738% (16/21682).

Table 2. Distribution of the gene encoding mitilectin (*mlc*) among MGS

Species	Number of strains	
	Total	*mlc*$^{+}$
S. mitis	164	41 (78-97% / 79-96%)*
S. pseudopneumoniae	90	50(95-100% / 94-100%)*
S. pneumoniae	21682	16 (95-97% / 94-96%)*

*(Nucleotide identity range of ORF / amino acid identity range of the product)

1.2 Phylogenetic analysis using a multi-locus sequence typing

In addition to SPpn, SM, and SPn, the homologous gene of *mlc* was also found in the two strains deposited as *S. oralis* subsp. *dentisani* on the database. However, these strains were suggested to be the strain of SM by the phylogenetic analysis using the multi-locus sequence typing (MLST) for the identification of SPn and their related species (Figure 2).

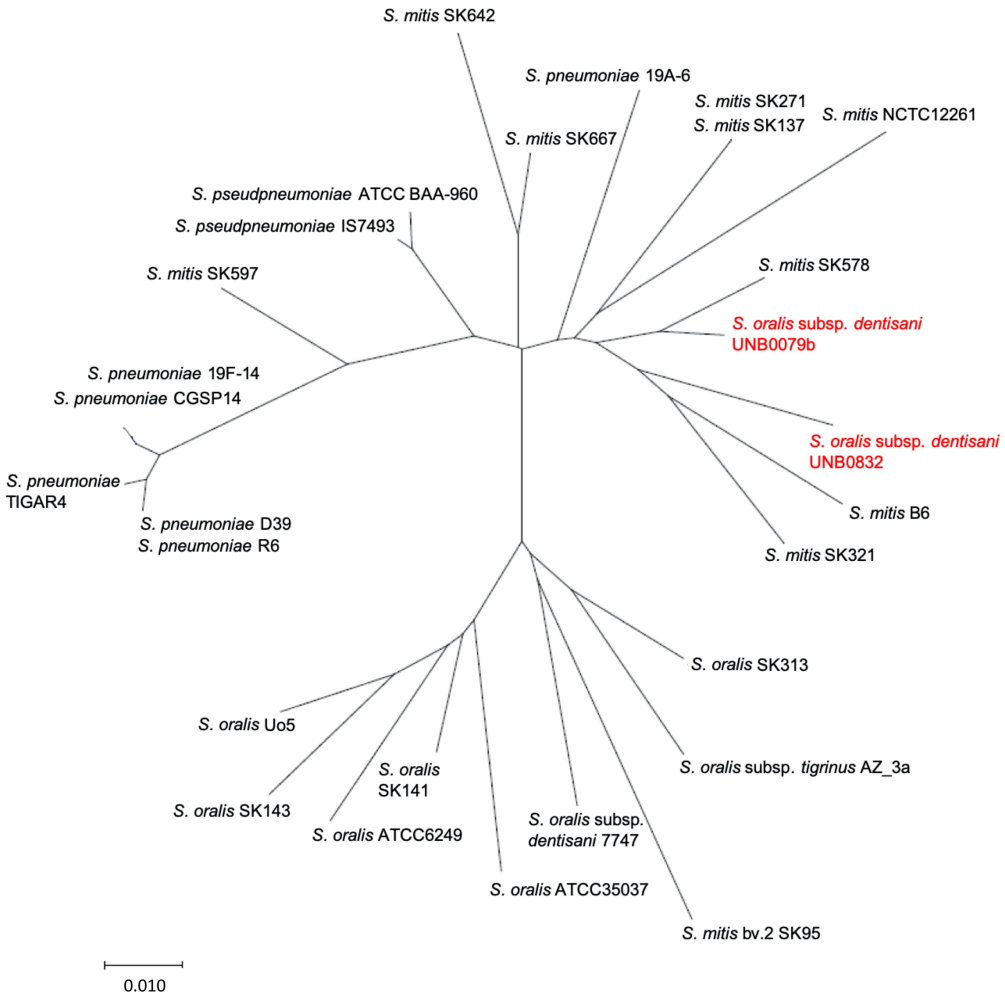

Figure 2. Phylogenetic tree of typical strains of *S. pneumoniae* (SPn), *S. mitis* (SM), *S. pseudopneumoniae* and *S. oralis* described based on the multi-locus sequence typing (MLST) for the identification of SPn. The two *mlc* gene-positive strains deposited as *S. oralis* subsp. *dentisani* UNB0079b and UNB0832 on the database was shown as red. These two strains were located in the clade of SM.

2. Preparation of recombinant mitilectins

The recombinants of full-length MLC (Cys-rMLC), four deletion mutants (ΔLF, ΔFT, ΔT, and ΔF), and a mutant with 6 point-mutations to alanine residues in the active-site residues for lectin activity (H509A, R536A, R543A, H643A, R670A, R678A) of the F5_F8_type_C domains (mutF) were prepared according to the method described in Materials and Methods. In all recombinants, His-tag and one Cys residue for the fluorophore labeling was added to the N-terminal side of the molecule (Figure 1).

The purified rMLC were electrophoresed by SDS-PAGE. As a result of CBB staining, the MLCs were purified with high purity (Figure 3). And the purified recombinant proteins were stored at -80 °C until the time of use.

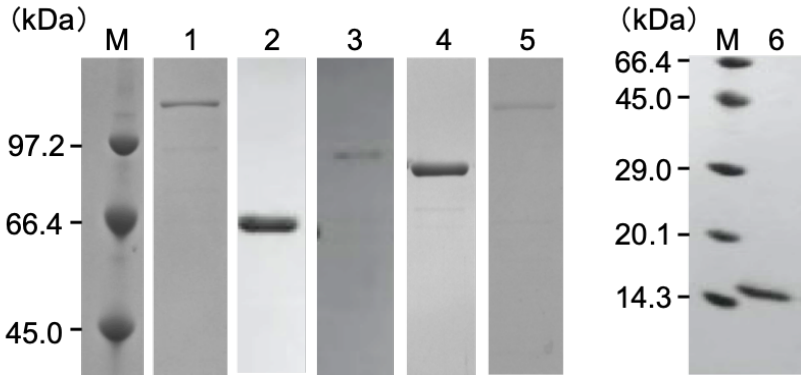

Figure 3. Coomassie Brilliant Blue stained image of the purified rMLCs. The N-terminal His-tagged recombinants possessing one Cys residue on their N-terminal for the fluorophore labeling was purified and stained by CBB after SDS-PAGE (1 μg/lane). Lanes: M, molecular weight marker; 1, Cys-rMLC (104.4 kDa); 2, ΔFT (53.8 kDa); 3, ΔT (86.2 kDa); 4, ΔF (69.5 kDa); 5, mutF (103.9 kDa); 6, ΔLF (13.3 kDa).

3. Detection of the mitilectin produced by the tested strains

3.1 Detection of the secreted mitilectin in the culture supernatant by immunoblotting

Culture supernatant of each MLC-producing strain ($SPpn^T$ and SM Nm-65) was

prepared and electrophoresed according to the method described in the Materials and Methods section. Both Nm-65 and SPpn^T were used because the present genome search revealed that Nm-65 had the *mlc* gene with 96% amino acid identity to that of SPpn^T. As a result of immunoblotting using α-MLC, a single band was detected in both culture supernatants of the MLC-producing strains (Figure 4, lanes 4 and 5) at the same position as the His-rMLC band (Figure 4, lanes 1–3). No band was detected in the culture supernatant of SM^T lacking the gene encoding MLC (Figure 4, lane 6). These results suggest that the MLC is secreted into the culture supernatant from strains possessing the MLC-encoding gene.

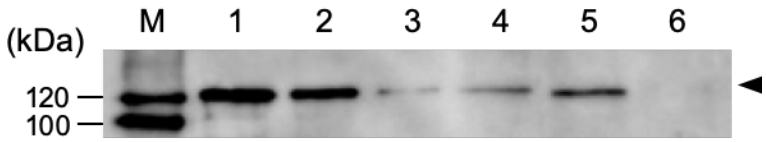

Figure 4. Immunoblotting image of MLC secreted from strains possessing *mlc*. Culture supernatant of the tested strains and His-rMLC for the positive control were applied to the SDS-PAGE and detected by immunoblotting using mouse antiserum against His-rMLC (α-MLC). The bands marked by arrowheads in lanes 4 and 5 indicate MLC secreted from the tested strains. Lanes: M, molecular weight marker; 1, His-rMLC (0.1 μg/lane); 2, His-rMLC (0.03 μg/lane); 3, His-rMLC (0.01 μg/lane); 4, *S. pseudopneumoniae*^{T} (SPpn^T); 5, *S. mitis* Nm-65 (Nm-65); 6, *S. mitis*^{T} (SM^T).

3.2 Detection of the mitilectin bound on the bacterial cell surface by enzyme-linked immunosorbent assay

The cell-surface bound type of MLC on the MLC-producing strains (SPpn^T and *S. mitis* Nm-65) was also investigated by ELISA using α-MLC for the first antibody of the detection system. As shown in Figure 5, a significant increase in absorbance (OD_{415}) of the substrate solution was observed for the MLC-producing strains SPpn^T (a) and Nm-65 (b) (black bars) compared to the control reaction using a non-immunized serum instead of α-MLC (white bars). Conversely, in SM^T lacking the MLC gene, no significant increase in

absorbance (OD_{415}) was observed, even in the reaction with α-MLC (SM^T, black bars). These results from the immunoblotting and ELISA suggested that the MLC produced from the strains possessing the MLC-encoding gene was found not only in the culture supernatant as the secreted form, but also on the bacterial cell surface as the cell-bound form. Each estimated MLC bound to $SPpn^T$ cells and Nm-65 cells using the calibration curve of His-rMLC was 11.3 ±1.79 [ng/50 μl of bacterial suspension (OD_{600}: 0.1)] and 19.7 ±1.75 [ng/50 μl of bacterial suspension (OD_{600}: 0.1)], respectively.

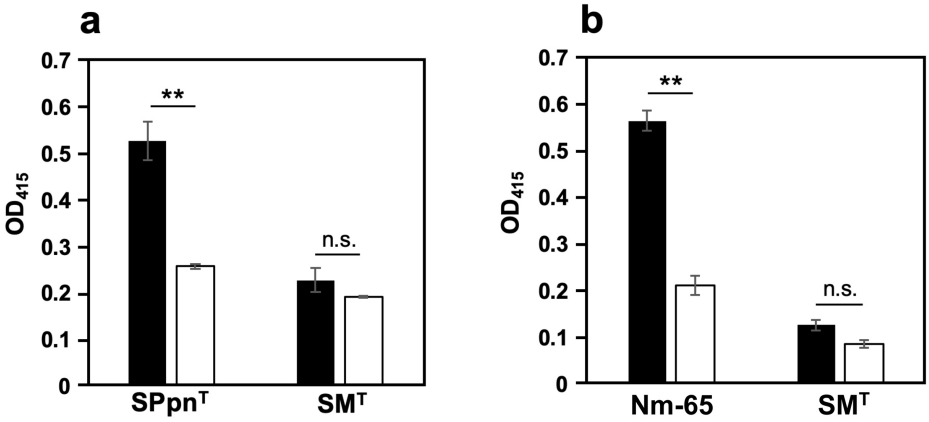

Figure 5. ELISA results for the assay of bound MLC on the bacterial cell surface. a, $SPpn^T$. **b**, Nm-65. MLC was detected by ELISA according to the method described in Materials and Methods. For the background control, non-MLC-producing strain SM^T was also used in the assay. The black and white bars show results using α-MLC and the non-immunized mouse serum as the primary antibody, respectively. Results are shown as the average of three independent experiments with standard deviation. Statistical evaluation was conducted by *t*-test (**: $p<0.01$. n.s.: not significant).

4. Characterization of the mitilectin function

4.1 Hemolytic activity of the recombinant mitilectins

The *mlc* gene is annotated as a gene encoding a CDC-related molecule with domain 4 that participates in the host cell-binding domain of CDC (21). However, the hemolytic activity of MLC was expected to be lost since MLC lacks domains 1-3 of typical CDC and unable to make pore on the cell membrane. In fact, no hemolytic activity was detected for His-rMLC even at a final concentration of 10 μg/mL in the reaction mixture, whereas other recombinant CDCs showed complete hemolysis at the concentration (Figure 6).

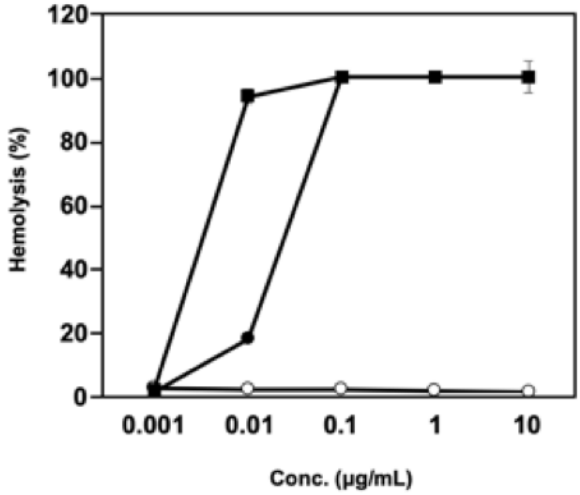

Figure 6. Measurement of hemolytic activity of His-rMLC. As the reference hemolysins, two recombinant CDCs (His-rSm-hPAF and His-rSLY) were used in the present assay. Each hemolytic reaction was performed in triplicate and the results are shown as mean values with SD. Open circles, His-rMLC; filled circles, His-rSm-hPAF; filled squares, His-rSLY.

4.2 Lipase activity of the recombinant mitilectins

The MLC molecule contained a lipase domain (lipase_3) and two of the three key residues in the active-site were conserved in the domain (Figure 7). Therefore, the lipase

activity of His-rMLC was measured using a commercially available kit. As a result, His-rMLC showed a significant lipase activity (0.99 nmol/min/ml) likely as the positive control (bovine milk lipoprotein lipase) of the kit, and the lipase activity of His-rMLC was decreased by the heat denaturation of His-rMLC (Figure 8, hdMLC).

```
MLC_lipase              ----QADDIRKVVGELAKDTSITKLYMTGHSLGGYLAQIAAVEAYQKYPDFYNHVLRKVT
Rat pancreatic lipase   RVVGAEIAFLVQVLSTEMGYSPENVHLIGHSLGAHVVGEAGRRLEGHVGRITGLDPAEPC
                                                      1

MLC_lipase              TFSAPKVITSRAVWNAENDFWDVGLESRKLAVSGKIKHYVVDNDNVVTPLIHNDRDIVTF
Rat pancreatic lipase   FQGLPEEVRLDPSDAMFVDVIHTDSAPIIPYLGFGMSQKVGHLDFFPNGGKEMPGCQKNI
                                          2

MLC_lipase              TGNSRFKHRSRGYFESRMNDILNFNI------
Rat pancreatic lipase   LSTIVDINGIWEGTQNFVACNHLRSYKYYASS
                                            3
```

Figure 7. Amino acid sequence alignment of lipase domain of MLC derived from SPpn^T and the rat pancreatic lipase (Protein Data Bank ID: 1BU8_A)**.** The orange-shaded amino acids (No. 1-No. 3) are predicted to be the conserved key residues composing active site for lipase activity.

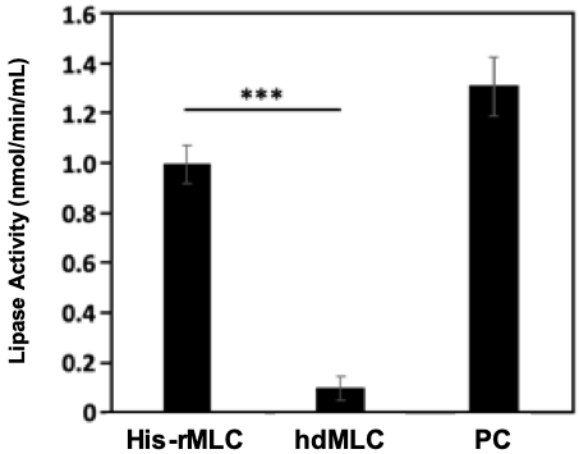

Figure 8. Measurement of the lipase activity of His-rMLC. The lipase activity of the His-rMLC derived from SPpn^T was measured using the Lipase Activity Assay Kit (Cayman Chemical). The assay was carried out in the reaction mixture containing His-rMLC or heat-denatured His-rMLC (hdMLC) at a final concentration of 0.1 μM in the reaction mixture, and the lipase activity was calculated according to the manufacturer's manual. For the positive control (PC), bovine milk lipoprotein lipase included in the kit was used. The results after subtraction of the background without His-rMLC were shown as the average of three independent experiments with standard deviation. Statistical evaluation was conducted by *t*-test (***: $p<0.005$).

4.3 Binding activity of the recombinant mitilectins to HL60 cells and HSC-2 cells

The binding of fluorescently labeled rMLC to human culture cell lines HL60 and HSC-2 was investigated based on the structural information that MLC possesses two types of potential binding domains: the tandem-arranged F5_F8_type_C domain, and the cell binding domain of CDC (domain 4).

In the investigation using a monocytic cell line, HL60, Cys-rMLC weakly bound to HL60 but most of them were easily dissociated by washing (Figure 9, refer to the green line and red line). On the other hand, Cys-rMLC showed significant binding to an oral squamous cell line, HSC-2 (Figure 10b). Interestingly, no cytotoxicity was induced in HSC-2 by Cys-rMLC. To reveal the domain responsible for the binding activity of rMLC, various rMLCs lacking the domain(s) in MLC (Figure 1) were prepared and compared the binding property of these mutants to that of Cys-rMLC. Consequently, only the mutant ΔT showed the maintained binding to HSC-2 cells (Figure 10d), and this binding was comparable to that of Cys-rMLC (Figure 10b). And it was noteworthy that the deletion of the tandem-arranged F5_F8_type_C domain caused a marked decrease on the binding activity of rMLCs to HSC-2 (Figures 10c, 10e and 10f).

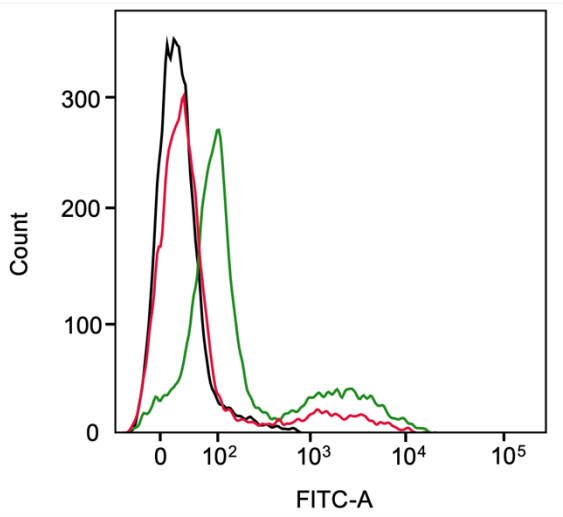

Figure 9. Binding property of the rMLCs to HL60 cells. N-terminal Alexa Fluor 488-labeled Cys-rMLC (final concentration, 0.1 μM) was incubated with HL60 cells and the fluorescent-labeled HL60 were detected using the FACSVerse. Black line, HL60 without incubation with Alexa Fluor 488-labeled rCys-MLC; Green line, HL60 incubated with Alexa Fluor 488-labeled Cys-rMLC; Red line, RPMI1640-washed HL60 after incubated with Alexa Fluor 488-labeled Cys-rMLCs.

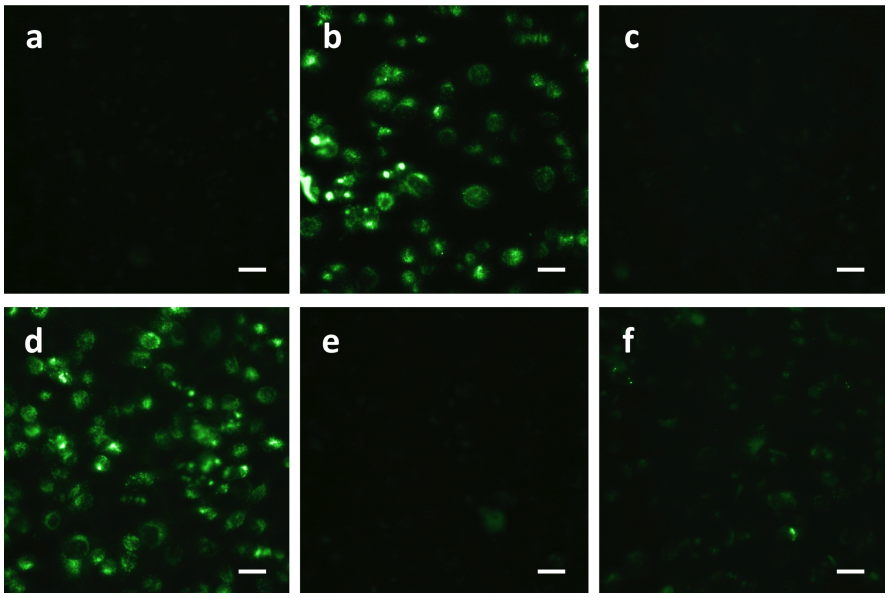

Figure 10. Domain-dependency of the binding activity of rMLCs to HSC-2 cells. Each N-terminal Alexa Fluor 488-labeled rMLC (final concentration, 0.1 μM) was incubated with HSC-2 cells. After co-incubation, unbound Alexa Fluor 488-labeled rMLCs were removed, and then incubated another overnight. Fluorescent images derived from Alexa Fluor 488-labeled rMLCs bound/incorporated to HSC-2 were observed using the IN Cell Analyzer 6000. The average HSC-2 cell number ± SD in this experiment (a-f) was 117.17 ±3.02 cells/field. Scale bars, 30μm. Samples: **a**, the sample of HSC-2 cells without any rMLCs or bacteria (nil); **b**, Alexa Fluor 488-labeled Cys-rMLC; **c**, Alexa Fluor 488-labeled ΔFT; **d**, Alexa Fluor 488-labeled ΔT; **e**, Alexa Fluor 488-labeled ΔLF; **f**, Alexa 488-labeled ΔF.

4.4 Contribution of the active site for lectin activity of mitilectin to the binding of HSC-2 cells

It was strongly suggested that rMLC binds to HSC-2 cells *via* the F5_F8_type_C domain(s) in the molecule (Figure 10). Moreover, as shown in Figure 11A, the active-site residues for lectin activity (6) is conserved in the F5_F8_type_C domains of MLC and LLY/Sm-hPAF. Therefore, molecular model of the tandem-arranged F5_F8_type_C domains derived from SPpn was constructed using the crystal structural data of the lectin domain of LLY (Figure 11B). Furthermore, investigation whether the active-site residues for lectin activity participate in the binding of MLC to HSC-2 cells was performed using another mutant of rMLC designated as mutF with 6 point-mutations to alanine residues in the active-site residues for lectin activity (H509A, R536A, R543A, H643A, R670A, R678A) of the F5_F8_type_C domains of MLC (Figure 11). Consequently, mutF showed a significant decrease in binding compared to the original rMLC (Cys-rMLC) (Figures 12Aa and 12Ab, and 12Ba and 12Bb). In addition, Cys-rMLC was bound to HSC-2 even after pre-incubation with the 5-fold excess molar of mutF (Figure 12Ac and 12Bc). On the other hand, in the case of HSC-2 pre-incubated with the 5-fold excess molar of Cys-rMLC, a similarly low binding found in the case of mutF without pre-incubation of Cys-rMLC was observed (Figure 12Ad and 12Bd).

A

```
                                                                1
MLC_SPpn_1        ----ENIALGKQVTQSSTAFGGDARRAVDG----NYDHNSVTHTNFQSKPWWQVDLAKEE
MLC_SPpn_2        ---AENIAWKKQVKKSSTVFEGDASYALDGITNSSYSQQSNTHTKSENQPWWEVDLGRTE
MLC_Nm-65_1       ----ENIALGKQVSQSSTAFGGDARRAVDGKVDGNYGHNSVTHTNFQSKPWWQVDLAKEE
MLC_Nm-65_2       ---AENIAWKKQAKQSSTDFGGDASRALDGNTNSSYSQQSITHTKFENQPWWEVDLGRTE
Sm-hPAF           PVEIENIARGKQASQSSTAYGGAATRAVDGNVDSDYGHHSVTHTNFEDNAWWQVDLGKTE
LLY               PVETENIARGKQASQSSTAYGGAATRAVDGNVDSDYGHHSVTHTNFEDNAWWQVDLGKTE
                      ****  **..:*** : * *  *:**    .*.::* ***: :.:.**:***.: *
                            2       3
MLC_SPpn_1        TIRQINIYNRTD-TAQDRLANFDVILLDSFGKEIERKRITSLK-DVSAQIAINYKRARYV
MLC_SPpn_2        QVGLVRLHNRGDGDVSKRLSDFDVILYDEKGTEVARQYVSKLDG-TSLDVQLNGKLGRRV
MLC_Nm-65_1       TIRQINIYNRTD-TAQDRLANFDVILLDSFGKEIERKRITSLK-DVSAQIAINHKKARYV
MLC_Nm-65_2       QVGLVRLHNRGDGELSKRLSDFDVILYDEKGTEVARQYVSKLDG-TSLDVQLNGKLGRRV
Sm-hPAF           NVGKVKLYNRGDGNVANRLSNFDVVLLNEAKKEVARQHFDSLNGKAELEVFFTAKDARYV
LLY               NVGKVKLYNRGDGNVANRLSNFDVVLLNEAKQEVARQHFDSLNGKAELEVFFTAKDARYV
                   :  :.::** *    .**::***:* :.   *: *: . .*.  .. :: :. * .* *

MLC_SPpn_1        RIELEGYN-----------
MLC_SPpn_2        RVQLRKNNQALSLAEVEVF
MLC_Nm-65_1       RIELEGYN-----------
MLC_Nm-65_2       RVQLRKNNQALSLAEVEVF
Sm-hPAF           KVELKTKNTPLSLAEVEVF
LLY               KVELKTKNTPLSLAEVEVF
                  :::*.  *
```

B

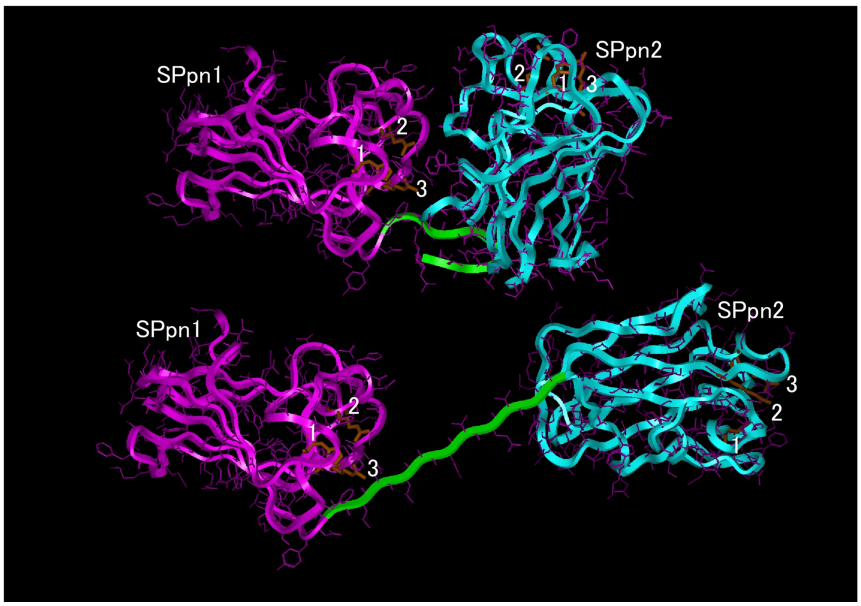

Figure 11. A. Amino acid sequence alignment of F5_F8_type_C domain of MLC derived from SPpn^{T} and *S. mitis* Nm-65, and of the lectin domain on the N-terminal of the 5-domain type CDC (Sm-hPAF and LLY). Two F5_F8_type_C domains of MLC located in tandem are shown as 1 and 2, respectively. Alignment of the amino acid sequence of F5_F8_type_C domain and the lectin domain was carried out using Clustal X. The orange-shaded amino acids (No. 1-No. 3) are predicted to be the conserved active-site residues for lectin activity. **B. Molecular model of tandem-arranged F5_F8_type_C domains of SPpn^{T} constructed using the crystal structural data of the lectin domain of LLY.** Upper; a molecular model with the contracted hinge peptide. Lower; a molecular model with the expanded hinge peptide. The F5_F8_type_C domains 1 and 2 are shown in magenta and cyan, respectively. The hinge peptide is shown in green. Three point-mutations at the deduced lectin active site residues in both F5_F8_type_C domains 1 and 2 are shown in **B** by numbers corresponding to No. 1-No. 3 in **A.**

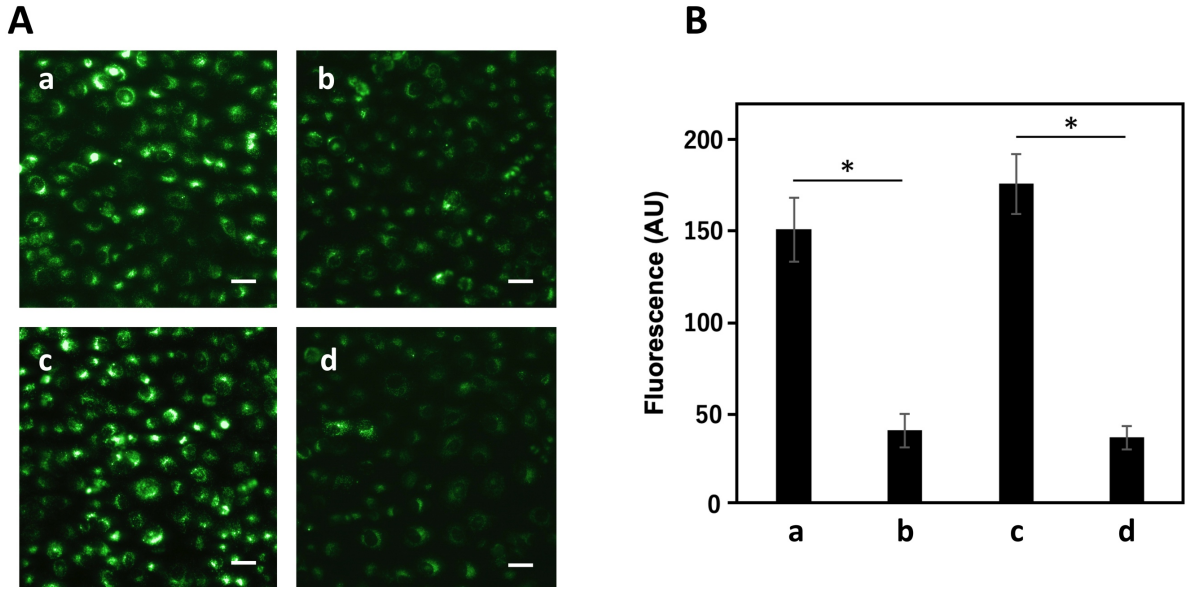

Figure 12. **Contribution of the predicted active site for lectin activity on the binding of MLC to human cells. A**. Fluorescent images of HSC-2 reacted with fluorescent-labeled rMLCs. Each 0.1 μM of Alexa Fluor 488-labeled Cys-rMLC or mutF was incubated with HSC-2 cells. The fluorescent images of HSC-2 cells were observed using the IN Cell Analyzer 6000. The average HSC-2 cell number ± SD in this experiment (a-d) was 121.00 ±9.53 cells/field. Scale bars showed 30 μm. **B**. Fluorescent intensity of the HSC-2 cell lysate. The measurement was carried out using a fluorescent microplate reader (excitation at 488 nm and emission at 530 nm). Results are shown as the average of the three independent experiments with standard deviation. Statistical evaluation was conducted by *t*-test (*: $p<0.05$). Samples: **a**, Alexa Fluor 488-labeled Cys-rMLC; **b**, Alexa Fluor 488-labeled mutF; **c**, Five-fold amount of non-labeled mutF was pre-incubated with HSC-2 cells, then Alexa Fluor 488-labeled Cys-rMLC was added; **d**, Five-fold amount of non-labeled Cys-rMLC was pre-incubated with HSC-2 cells, then Alexa Fluor 488-labeled mutF was added.

5. Characterization of the mitilectin-producing bacterial strains

5.1 Mitilectin-dependent binding of mitilectin-producing strains to HSC-2 cells

We also investigated whether MLC facilitates the binding of MLC-producing bacteria to target cells using the fluorescent-labeled bacterial cells with the efficiency of fluorescent labeling was almost the same. From results shown in Figures 13A and 13B, MLC-producing strains, SPpn^{T} and *S. mitis* Nm-65, showed apparent binding to HSC-2 cells by 3 h culture (w/o serum in Figure 13A) without remarkable cytotoxicity. This binding was

significantly decreased in the presence of α-MLC (w/α-MLC in Figure 13A). On the other hand, no inhibitory effect was observed in the presence of non-immunized mouse serum (w/non-immune in Figure 13A). In the case of non-MLC-producing strain SM^T, which showed less binding than MLC-producing SM strain Nm-65, no significant decrease in binding to HSC-2 cells was observed, even in the presence of either α-MLC or non-immunized mouse serum (Figure 13).

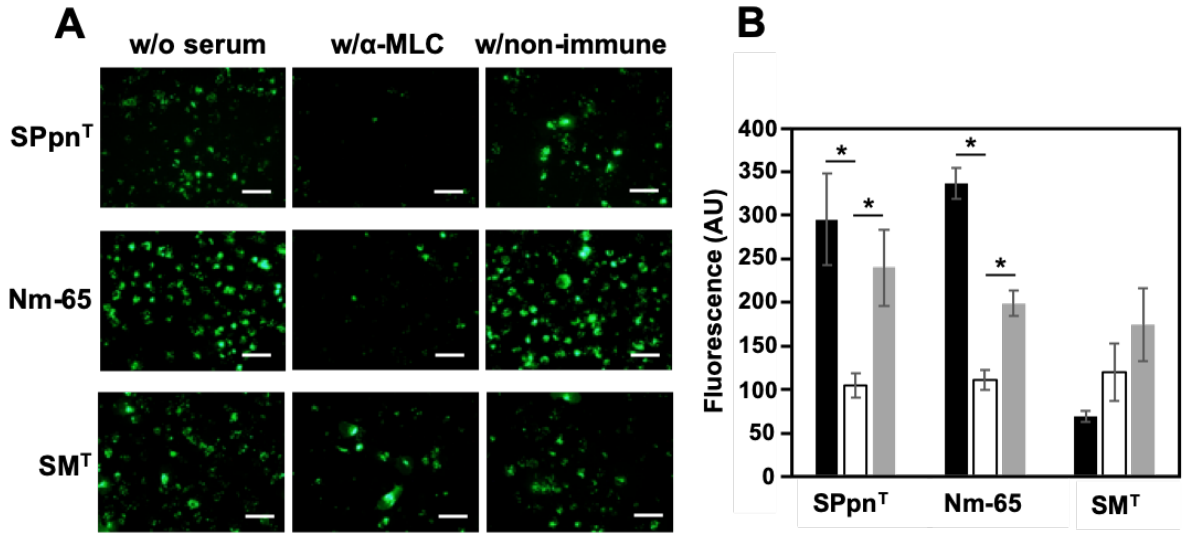

Figure 13. **MLC-dependent binding of MLC-producing strains to HSC-2 cells.** Each of the tested strains was labeled using PKH67 Green Fluorescent Cell Linker Midi Kit, then co-cultivated with HSC-2 cells at multiplicity of infection (MOI) =100. This investigation was also conducted using the bacteria pre-incubated with α-MLC or non-immune serum prior to co-cultivation with HSC-2 cells. The average HSC-2 cell number ± SD in this experiment was 109.33 ±11.85 cells/field. **A**. Fluorescent images of HSC-2 cells with PKH67-labeled bacteria observed by Olympus IX71 fluorescence microscope equipped with DP72 (Olympus). Scale bars indicate 50 μm. **B**. Fluorescent intensity of the HSC-2 cell lysate. The measurement was carried out using a fluorescent microplate reader (excitation at 480 nm and emission at 530 nm). The black bars, white bars, and gray bars show the fluorescence intensity of HSC-2 cells incubated with the bacteria without serum treatment, treated by α-MLC, and treated by non-immune serum, respectively. Results are shown as the average of three independent experiments with standard deviation. Statistical evaluation was conducted by *t*-test (*: $p<0.05$).

5.2 Binding of the gene deletion mutant encoding mitilectin derived from *Streptococcus mitis* strain Nm-65 to HSC-2 cells

The *mlc*-delection mutant of Nm-65 (Δ*mlc*) that showed comparative growth relative to the wildtype strain (WT) was constructed as described in "Materials and Methods." The growth curves of both strains were shown in Figure 14. Its host-cell-binding activity was compared with that of WT using the bacterial cells of tested strains with almost the same efficiency of fluorescent labeling. As shown in Figure 15, the binding activity of Δ*mlc* was considerably lower than that of WT, but was not completely lost.

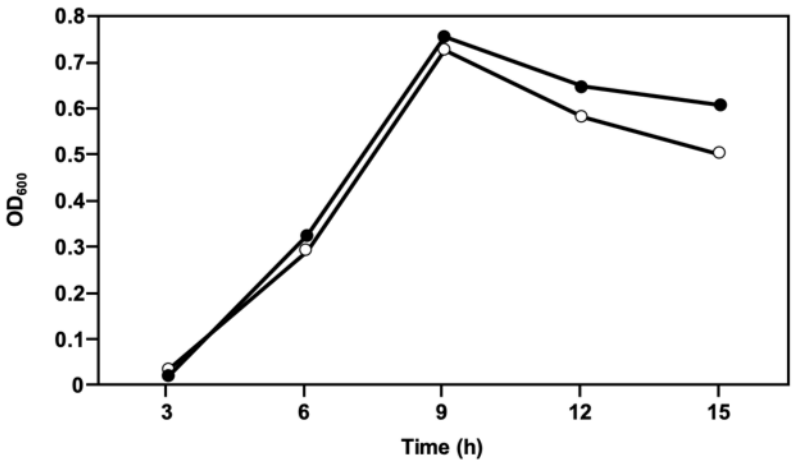

Figure 14. The growth curves of the wildtype strain (WT) and *mlc*-deleted mutant of Nm-65. Open circles, WT; filled circles, *mlc*-deleted mutant. Representative results of the experiments considered twice are shown.

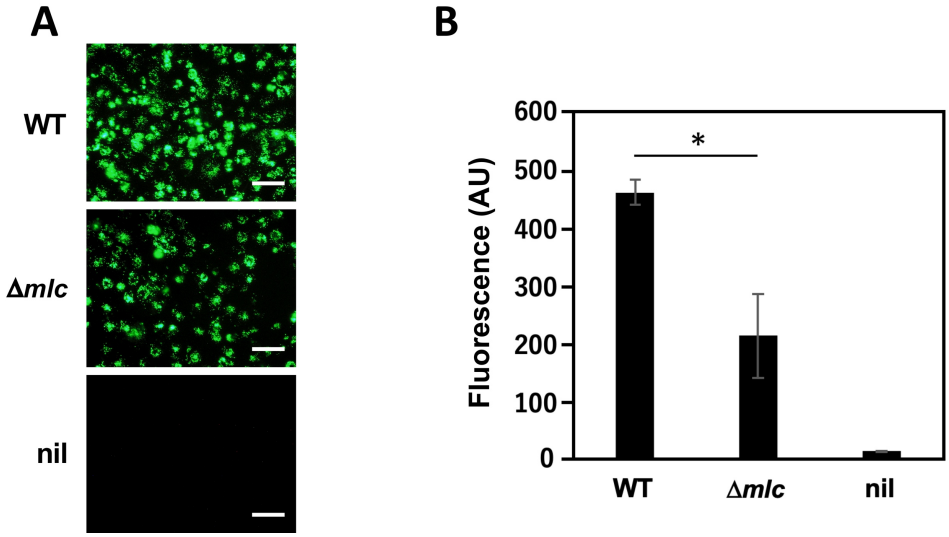

Figure 15. **Inhibitory effect of *mlc*-deletion on binding of Nm-65 to HSC-2 cells.** The binding of tested strains to HSC-2 cells was evaluated according to the same method described for Figure 13. **A**. Fluorescent images of PKH67-labeled bacteria associated with HSC-2 cells observed by Olympus IX71 fluorescence microscope equipped with DP72 (Olympus). Scale bars indicate 50 µm. **B**. Fluorescent intensity of the HSC-2 cell lysate. The measurement was carried out using a fluorescent microplate reader (excitation at 480 nm and emission at 530 nm). Results are shown as the average of three independent experiments with standard deviation. Statistical evaluation was conducted by *t*-test (*: $p<0.05$).

CHAPTER 5. Discussion

Recently, the gene encoding a novel molecule composed of the part of the domains of reported CDC (tandem-arranged lectin domains and the receptor recognition domain called domain 4) and the deduced lipase domain, designated as mitilectin (MLC) in this study, was shown in the genome of SPpn strain IS7493 (21). In this study, the distribution of the gene encoding MLC among the strains belonging to MGS, the molecular functions of MLC, and the contribution of MLC to the pathogenicity of the strains/species were focused and investigated.

As first, the distribution of the gene encoding MLC on the genome of various species of streptococci (20 species total) was investigated and revealed that many strains possessing this gene were found in the two species belonging to MGS, SPpn (gene-positive rate, 55.6%) and SM (gene-positive rate, 25.0%) in the search (Table 2). Though 16 strains belonging to SPn were found as the *mlc*-gene positive strain, the positive rate of *mlc*-gene in SPn searched in this study is only 0.0738%. In addition, other two strains deposited as *S. oralis* subsp. *dentisani* were revealed to possess the *mlc*-gene, however, these two strains are thought to be SM according to our MLST analysis (Figure 2). Such information suggests that the gene encoding MLC is conserved mainly in the strains of both SPpn and SM species with relatively higher rate compared to the other species belonging to MGS. The strains of three species such as SPpn, SM, and SPn among MGS are closely related based on the genetic information (10, 18). In addition, the strains of SPn and SM show the natural transformation utilizing a similar competence system induced by the competence-stimulating peptide (CSP) (31). According to these findings, it was suggested that the distribution/transmission of the *mlc* gene among the strains belonging to SM, SPn, and also SPpn may occur due to natural transformation in these species.

As mentioned, MLC has the potential for multiple functions, such as lipase activity, lectin activity, and pore-forming activity on erythrocytes from the information of deduced structural domains. In order to investigate the molecular functions of MLC, several recombinant proteins of MLC (rMLC), including some of domain-deleted mutants, were prepared and used. At first, the pore-forming activity of His-rMLC toward human erythrocytes was tested, but no hemolysis was detected (Figure 6). This result indicated that some domains related to the CDC (F5_F8_type_C domain and thiol cytolysin domain) in MLC are insufficient or not functional to form a pore on the cell membrane. Next, significant lipase activity (0.99 nmol/min/ml) was shown (Figure 8) though one residue of the deduced lipase active triad was lacking (Figure 7). According to these facts, it is suggested that unidentified amino acid(s) participate in the formation of the actual active site of the lipase domain in rMLC and make it functional. Though this lipase activity may contribute to utilization of glycerides in MLC-producing strains, it has not been clarified how this lipase activity participates in the growth or pathogenicity of MLC-producing strains.

From the result of Figure 10, fluorescently labeled Cys-rMLC showed significant binding to HSC-2 cells without detectable cytotoxicity. Moreover, because only the ΔT mutant retained the binding activity to HSC-2 cells comparable to full-length rMLC (Cys-rMLC), and all mutants lacking tandem-arranged F5_F8_type_C domain lost binding activity, it is suggested that the MLC would bind to HSC-2 cells not *via* thiol cytolysin domain for cell membrane binding, but instead *via* the tandem-arranged F5_F8_type_C domains. A molecular model of the tandem-arranged F5_F8_type_C domains was constructed using the crystal structural data of the lectin domain of LLY (3LE0) by homology modeling (Figure 11B). The hinge region between each F5_F8_type_C domain, ALSLAEVQVYR, will functioned as a flexible linker with expanding and contracting ability that increases the accessibility of the binding sites in F5_F8_type_C domain to the receptor on host cell surface. In order to clarify the role of lectin activity in MLC binding, further investigation was

conducted using a mutant of MLC with six Ala-substitutions of lectin active sites in the F5_F8_type_C domain. Experimental results strongly supported the idea that fluorescent-labeled Cys-rMLC can bind to HSC-2 cells through the lectin activity of the F5_F8_type_C domain (Figure 12). Similar binding activity of rMLC *via* the F5_F8_type_C domain has also been observed in human lung carcinoma cell line A549 (data not shown), so the observed binding of rMLC to human cells *via* the F5_F8_type_C domain is not restricted to HSC-2 cells. Taken together of the above results, MLC is a multifunctional protein with lipase activity and cell membrane-binding activity, presumably *via* lectin activity.

MLC secreted from $SPpn^T$ is present not only in the culture supernatant, but also on the bacterial cell surface (Figure 4 and 5). In addition, the bacterial cell-surface-bound MLC of $SPpn^T$ contributed to the bacterial cells binding of HSC-2 cells (Figure 13). A similar observation was previously reported for intermedilysin (ILY), a CDC secreted from *Streptococcus intermedius* (32). This report suggested that ILY may induce the bacterial invasion by promoting interactions between bacteria and host cells. Therefore, MLC bound to the bacterial cell surface may contribute to the potential pathogenicity of MLC-producing strains to human cells in a similar way.

From the result of genomic search for the possession of *mlc*-gene *in silico*, the presence of *mlc* on the genome was not restricted in the species of SPpn, and *mlc*-gene was also distributed to the other species belonging to MGS, such as SM and SPn (Table 2). One of the strains of SM, Nm-65 isolated from a patient with Kawasaki Disease (23), also possessed the *mlc* gene, and the produced MLC was detected both in the culture supernatant and on the cell-surface-bound form, similar to the $SPpn^T$ (Figure 4 and 5). Moreover, the MLC-dependent binding of Nm-65 to HSC-2 cells was also observed (Figure 13). According to these results, the molecular function of MLC may be highly conserved among the MLC-producing strains regardless of the species, at least in SM. Fortunately, the experimental system for the transformation of Nm-65 was established recently (29). Using this system, the

mlc-deletion mutant derived from Nm-65 (Δ*mlc*) was constructed, and the characteristic of this mutant was investigated. As shown in Figure 15, the apparent decrease in binding of the tested bacteria to HSC-2 cells was observed compared to the results in the parent strain (WT), although half of the binding was retained in Δ*mlc* strain. This result also strongly suggested that a large part of the binding of the MLC-producing strains to host cells is facilitated or stabilized by MLC produced. Therefore, further investigation to clarify the receptor(s) with glycochain(s) specific for the MLC should be pursued.

In the present study, the molecular functions of the deduced multifunctional protein MLC were investigated. The findings in this study provide the novel information regarding MLC, especially its function as a cell adhesion molecule. According to the information including our ongoing investigation, the molecular characteristics of the multifunctional MLC will be important for the consideration of potential pathogenicity about the strains in MGS that producing the MLC.

CHAPTER 6. Conclusion

In contrast with the typical human pathogenic streptococci such as *Streptococcus pyogenes* and *S. pneumoniae*, enough investigations about the species belonging to MGS except for *S. pneumoniae* that enable to consider their pathogenicity has not yet been carried out. However, the information from some reports published in the recent years (13-17) suggests that the species of SPpn and SM, generally recognized as an opportunistic pathogen of human, may show the potential pathogenicity. Therefore, we have been focused and investigated on these species. Consequently, previous studies have confirmed the structural and functional diversity of the CDCs possessed by MGS species (5, 7, 8).

In the present study, the newly reported CDC-related molecule named MLC was investigated: We searched for strains carrying the *mlc* gene and performed functional analysis of MLC using recombinant proteins. Moreover, we investigated the contribution to pathogenicity, including the assay for molecular localization of MLC on the bacterial cells. According to the results described in this study, the strains possessing the *mlc* gene was mainly observed in two species, SPpn and SM. With regard to the molecular functions of MLC, it was revealed that MLC produced by the *mlc* gene-positive strain is a multifunctional protein with lectin and lipase activities but no cytotoxic activity and functions as an adhesion molecule participating in the bacterial binding to the host human cells *via* its lectin domain(s). Interestingly, it has also been confirmed that the strains possessing the *mlc* gene also carry the gene(s) encoding CDCs based on the genomic analysis. This *in silico* information is suggesting that the MLC-dependent adhesion would enhance the cytotoxicity by CDCs and may contribute to the pathogenicity of MLC-producing strains.

This study is meaningful as the first research on MLC to unveil the true pathogenicity of the opportunistic pathogens belonging to MGS such as SPpn and SM. As the future work of this study, the search of the cellular receptor(s) for MLC and the investigation

for the mechanism(s) of the mode of action of MLC to the target human cells should be carried out to complete the characterization of MLC. Further successful progress is expected in near future.

ACKNOWLEDGMENTS

I especially appreciate my supervisor Professor Hideaki Nagamune for his valuable ideas, instructions and suggestions on my research for years and Associate Professor Toshifumi Tomoyasu for his kind support and constructive advices on my experiments, as well as Lecturer Atsushi Tabata for providing experimental guidance and helpful opinions. I equally thank Prof. Kazuto Ohkura (Suzuka University of Medical Science) for molecular modeling. I would like to show my gratitude to Professor Emeritus of Nippon Medical College Hisashi Ohkuni (Health Science Research Institute East Japan), Assistant Professor Ayuko Takao (Tsurumi University), and Professor Ken Kikuchi (Tokyo Women's Medical University) for the kind gift of bacterial strains. I am also grateful to the undergraduate student Mr. Hiroki Oda and graduate student Ms. Chihiro Kodama in our laboratory for their support of investigation.

Finally, I wish to express my sincere appreciation to my family and friends for their attention, support and encouragement.

REFERENCES

[1] Heuck AP, Moe PC, Johnson BB. The cholesterol-dependent cytolysin family of gram-positive bacterial toxins. Subcell Biochem. 2010; 41:551-577.

[2] Ramachandran R, Tweten RK, Johnson AE. The domains of a cholesterol-dependent cytolysin undergo a major FRET-detected rearrangement during pone formation. Proc Natl Acad Sci USA. 2005; 102:7139-7144.

[3] Hotze EM, Wilson-Kubalek E, Farrand AJ, Bentsen L, Parker MW, Johnson AE, Tweten RK. Monomer-monomer interactions propagate structural transitions necessary for pore formation by the cholesterol-dependent cytolysins. J Biol Chem. 2012; 287:24534-24543.

[4] Soltani CE, Hotze EM, Johnson AE, Tweten RK. Specific protein-membrane contacts are required for prepore and pone assembly by a cholesterol-dependent cytolysin. J Biol Chem. 2007; 282:15709-15716.

[5] Ohkuni H, Nagamune H, Ozaki N, Tabata A, Todome Y, Watanabe Y, Takahashi H, Ohkura K, Kourai H, Ohtsuka H, Fischetti VA, Zabriskie JB. Characterization of recombinant *Streptococcus mitis*-derived human platelet aggregation factor. APMIS. 2012; 120:56-71.

[6] Farrand S, Hotze E, Friese P, Hollingshead SK, Smith DF, Cummings RD, Dale GL, Tweten RK. Characterization of a Streptococcal cholesterol-dependent cytolysin with a Lewis y and b specific lectin domain. Biochemistry. 2008; 47:7097-7107.

[7] Tabata A, Ohkura Kazuto, Ohkubo Y, Tomoyasu T, Ohkuni H, Whiley RA, Nagamune H. The diversity of receptor recognition in cholesterol-dependent cytolysins. Microbiol Immunol. 2014; 58:155-171.

[8] Kawaguchi Y, Tabata A, Nagamune H, Ohkura K. Profiles of ILY, VLY and Sm-hPAF interaction with human CD59. Anticancer Res. 2013; 33:2901-2904.

[9] Arbique JC, Poyart C, Trieu-Cuot P, Quesne G, Carvalho Mda G, Steigerwalt AG, Morey RE, Jackson D, Davidson RJ, Facklam RR. Accuracy of phenotypic and genotypic testing for identification of *Streptococcus pneumoniae* and description of *Streptococcus pseudopneumoniae* sp. nov. J Clin Microbiol. 2004; 42:4686-4696.

[10] Shahinas D, Thornton CS, Tamber GS, Arya G, Wong A, Jamieson FB, Ma JH, Alexander DC, Low DE, Pillai DR. Comparative genomic analyses of *Streptococcus pseudopneumoniae* provide insight into virulence and commensalism dynamics. PLoS One. 2013; 8:e65670.

[11] Mitchell TJ. The pathogenesis of streptococcal infections: from tooth decay to meningitis. Nat Rev Microbiol. 2003; 1:219-230.

[12] Weiser JN, Ferreira DM, Paton JC. *Streptococcus pneumoniae*: transmission, colonization and invasion. Nat Rev Microbiol. 2018; 16:355-367.

[13] Mizuno M, Ito Y, Masuda T, Toda S, Hiramatsu H, Suzuki Y, Ozaki T, Yasuda Y, Ito I, Tsuboi N, Sato W, Maruyama S, Imai E, Matsuo S. A case of fulminant peritonitis caused

by *Streptococcus mitis* in a patient on peritoneal dialysis. Intern Med. 2011; 50:471-474.

[14] Matsui M, Ito M, Kuramae H, Inukai T, Sakai A, Okugawa M. Infective endocarditis caused by multidrug-resistant *Streptococcus mitis* in a combined immunocompromised patient: an autopsy case report. J Infect Chemother. 2013; 19**:**321-325.

[15] Fuursted K, Littauer PJ, Greve T, Scholz CFP. Septicemia with *Streptococcus pseudopneumoniae*: report of three cases with an apparent hepatic or bile duct association. Infect Dis. 2016; 48:636-639.

[16] Harf-Monteil C, Granello C, Le Brun C, Monteil H, Riegel P. Incidence and pathogenic effect of *Streptococcus pseudopneumoniae.* J Clin Microbiol. 2006; 44:2240-2241.

[17] Keith ER, Podmore RG, Anderson TP, Murdoch DR. Characteristics of *Streptococcus pseudopneumoniae* isolated from purulent sputum samples. J Clin Microbiol. 2006; 44:923-927.

[18] Garriss G, Nannapaneni P, Simões AS, Browall S, Subramanian K, Sá-Leão R, Goossens H, de Lencastre H, Henriques-Normark B. Genomic characterization of the emerging pathogen *Streptococcus pseudopneumoniae*. mBio. 2019; 10:e01286-19.

[19] Nishimoto AT, Rosch JW, Tuomanen EI. Pneumolysin: Pathogenesis and therapeutic target. Front Microbiol. 2020; 11:1543.

[20] Johnston C, Hinds J, Smith A, van der Linden M, Van Eldere J, Mitchell TJ. Detection of large numbers of pneumococcal virulence genes in streptococci of the mitis group. J Clin Microbiol. 2010; 48:2762-2769.

[21] Morales M, Martin-Galiano AJ, Domenech M, Garcia E. Insights into the evolutionary relationships of LytA autolysin and Ply pneumolysin-like genes in *Streptococcus pneumoniae* and related Streptococci. Genome Biol Evol. 2015; 7:2747-2761.

[22] Enright MC, Spratt BG. A multilocus sequence typing scheme for *Streptococcus pneumoniae*: identification of clones associated with serious invasive disease. Microbiology. 1998; 144:3049-3060.

[23] Ohkuni H, Todome Y, Okibayashi F, Watanabe Y, Ohtani N, Ishikawa T, Asano G, Kotani S. Purification and partial characterization of a novel human platelet aggregation factor in the extracellular products of *Streptococcus mitis*, strain Nm-65. Immunol Med Microbiol. 1997; 17:121-129.

[24] Tabata A, Ohkubo Y, Sakakura E, Tomoyasu T, Ohkura K, Nagamune H. Investigation of a bacterial pore-forming chimera toxin for application as a novel drug-delivery system tool. Anticancer Res. 2012; 32:2323-2329.

[25] Ohkuni H, Nagamune H, Ozaki N, Tabata A, Todome Y, Watanabe Y, Takahashi H, Ohkura K, Kourai H, Ohtsuka H, Fischetti VA, Zabriskie JB. Characterization of recombinant *Streptococcus mitis*-derived human platelet aggregation factor. APMIS. 2012; 120:56-71.

[26] Nagamune H, Ohnishi C, Katsuura A, Fushitani K, Robert AW, Tsuji A, Matsuda Y. Intermedilysin, a Novel cytotoxin specific for human cells, secreted by *Streptococcus*

intermedius UNS46 isolated from a human liver abscess. Infect Immun. 1996; 64:3093-3100.

[27] Ohkura K, Nagamune H, Kourai H. Structural analysis of human specific cytolysin intermedilysin aiming application to cancer immunotherapy. Anticancer Res. 2004; 24:3343-3354.

[28] Ohkura K, Hori H, Nagamune H. Molecular dynamics of human-specific cytolysin: Analysis of membrane binding motif for therapeutic application. Anticancer Res. 2006; 26:4055-4062.

[29] Tabata A, Ohkuni H, Saigo T, Kodama C, Tang Q, Tomoyasu T, Fukunaga Y, Itoh Y, Nagamune H. Cytotoxic property of *Streptococcus mitis* strain producing two different types of cholesterol-dependent cytolysins. Infect Genet Evol. 2020; 85:104483.

[30] Takamatsu D, Arai R, Akiyama TM, Okumura K, Okura M, Kirikae T, Kojima A. Identification of mutations involved in the requirement of potassium for growth of typical *Melissococcus plutonius* strains. Appl Environ Microbiol. 2013; 79:3882-3886.

[31] Salvadori G, Junges R, Morrison DA, Petersen FC. Competence in *Streptococcus pneumoniae* and close commensal relatives: Mechanisms and implications. Front Cell Infect Microbiol. 2019; 9:94.

[32] Sukeno A, Nagamune H, Robert AW, Syed IJ, Joseph AO, Ohkura K, Maeda T, Hirota K, Miyake Y, Kourai H. Intermedilysin is essential for the invasion of hepatoma HepG2 cells by *Streptococcus intermedius*. Microbiol Immunol. 2005; 49:681-694.

LIST OF PUBLICATION

I. **Airi Matsumoto,** Atsushi Tabata, Kazuto Ohkura, Hiroki Oda, Chihiro Kodama, Hisashi Ohkuni, Ayuko Takao, Ken Kikuchi, Toshifumi Tomoyasu and Hideaki Nagamune. Molecular characteristics of an adhesion molecule containing cholesterol-dependent cytolysin-motif produced by Mitis group streptococci. *Microbiol Immunol*. 2020
Doi: 10.1111/1348-0421.12868